EASR

Engineering and Applied Science Research

https://www.tci-thaijo.org/index.php/easr/index

Published by the Faculty of Engineering, Khon Kaen University, Thailand

Silver nanoparticle synthesis using the serum obtained after rubber coagulation of skim natural rubber latex with chitosan solution

Thanaporn Jullabuth and Panu Danwanichakul*

Department of Chemical Engineering, Faculty of Engineering, Thammasat University, Rangsit Campus, Klong-Luang, Pathumthani 12120, Thailand

Received 11 August 2020
Revised 10 December 2020
Accepted 21 December 2020

Abstract

This research focused on a green synthesis of silver nanoparticles (AgNPs) using the serum from skim natural rubber latex (SNRL), which is simple and low cost. Chitosan in acetic acid was used as a coagulant to remove rubber particles from SNRL. This leftover serum was diluted with the same amount of water and used as a source of reducing agent in the synthesis of AgNPs. The effects of NaOH and $AgNO_3$ concentrations were studied. The AgNP colloids were characterized by UV-vis spectrophotometry and transmission electron microscopy. Three AgNP samples were chosen and tested for their sensing ability when reacting with H_2O_2. The results showed that increasing NaOH concentration from 0.1 M to 1 M caused the absorbance peak to shift to a lower wavelength, implying that the AgNPs were smaller; the opposite trend was observed when increasing $AgNO_3$ concentration from 1 to 3 mM. From these samples, three were chosen based on clear differences in absorbance peak positions, which were at 405, 417 and 424 nm, consistent with average sizes of 7.942, 8.464 and 9.284 nm with SDs of 4.000, 1.673, and 1.941 nm, respectively. In the test of sensing ability of AgNPs when reacting with H_2O_2, it was necessary to enhance the stability of diluted AgNP samples with 5 wt % polyethylene glycol. The three AgNP samples were reacted with H_2O_2 at various concentrations from 0.0625 to 0.5 mM. The AgNPs of small sizes yielded high sensitivity provided that the colloidal stability was adequate.

Keywords: Green synthesis, Silver nanoparticles, Skim natural rubber latex, Chitosan, Hydrogen peroxide, Sensor

1. Introduction

The green synthesis of different types of metallic nanoparticles has been extensively studied and still attracts much attention. For example, silver nanoparticles (AgNPs) [1-3], gold nanoparticles (AuNPs) [4-7], nickel nanoparticles (NiNPs) [8, 9], and magnetic nanoparticles (FeNPs) [10, 11] have been investigated. Among these, AgNPs are very popular due to their many interesting characteristics, including their ability to inhibit the bacterial growth, good catalytic activity, optical properties and low cost [12]. As a result, AgNPs can be applied as bacterial inhibitive agents, biosensors and chemical sensors [13-15].

The green synthesis of nanoparticles includes both the use of plant extracts such as *Lysiloma acapulcensis* [16], *Melia azedarach* [17], and *Nigella sativa* [18] and waste produced from various manufacturing processes such as rubber coagulation processes [19]. The fresh latex, with approximately 30 wt % dry rubber content (DRC), is centrifuged to obtain the concentrated latex with about 60 wt % DRC and the skim natural rubber latex (SNRL) with about 3-8 wt % DRC. Ammonia is added to the fresh latex before centrifugation to prevent bacterial attack and to increase the colloidal stability of the rubber particles. Usually, the rubber particles in the SNRL with leftover ammonia are coagulated using sulfuric acid at a high concentration, yielding low-grade solid rubber and leaving a serum as a waste to be treated. On the basis of 5% DRC, the serum contains mostly water and approximately 3.25 wt % proteins, 0.425 wt % lipid, and 3.125 wt % carbohydrates/sugar (L-quebrachitol, sucrose, glucose, fructose, raffinose and two pentoses) [20, 21]. Some of these substances, such as glucose, fructose, pentoses, fatty acids and the leftover ammonia could be used as reducing agents for the synthesis of metallic nanoparticles.

Early attempts were made to use SNRL directly in the synthesis of AgNPs and the obtained AgNPs tested for their anti-bacterial activity [22]. A coating layer of rubber on the AgNPs was observed by transmission electron microscopy (TEM), which might result in low anti-bacterial activity of the samples. Later, the concentration of ammonia in SNRL was shown to affect the size of the AgNPs [23]. Another work reported the use of AgNPs synthesized in SNRL to increase the efficiency of dye-sensitized solar cells by 58.9% [24].

With the concern about the interference of negatively charged rubber particles in SNRL with positive metallic ions during the synthesis of nanoparticles, especially for higher-valence metallic ions such as gold ions, our later studies focused on the use of only the serum in the synthesis. Since coagulation with sulfuric acid at a high concentration affects the environment and the quality of the rubber, some researchers have aimed to replace sulfuric acid with more environmentally friendly coagulants [25]. Therefore, different coagulants that partly remain in the serum could have some effects on the syntheses.

*Corresponding author. Tel.: +66 2564 3001
Email address: dpanu@engr.tu.ac.th
doi: 10.14456/easr.2021.45

The serums from SNRL with various remaining coagulants-H_2SO_4, CH_3COOH, and cationic polyacrylamide (PAM) solutions-were investigated for their potential use as sources of reducing agents in the green synthesis of AuNPs [26]. The results showed that the serum with H_2SO_4 resulted in large particles, while the serums with both CH_3COOH and PAM could stabilize the AuNPs.

Chitosan is derived from chitin, which is the second most abundant biopolymer in nature and found in animals with a hard carapace and jointed legs, such as shrimps, crayfish and crabs. Chitosan is protonated to become positively charged when dissolved in weak acids or water. It dissolves well in organic acids with a pH of less than 6.5 [27]. Highly positively charged chitosan could make an effective coagulant to remove the negatively charged rubber particles in SNRL, leaving the remaining serum containing organic material, including an amount of chitosan. Up to now, there has been no research into the system of nanoparticle synthesis using the serum obtained from coagulation with chitosan in acetic acid. This system is of interest from the aspect of better quality of both wastewater and coagulated rubber, as reported by Werathirachot and Danwanichakul [28] who compared it to the conventional sulfuric acid system.

In addition, the chemical sensing application of AgNPs synthesized from the serum was also studied in this work. The chosen chemical was hydrogen peroxide (H_2O_2). The quantification of H_2O_2 is a subject of interest because it is a product of a variety of reactions [29] and is normally used in reactions involving strong oxidizing agents [30-32]. There are many detection methods for H_2O_2, such as spectrophotometry [33], chemiluminescence [34, 35], electrochemistry [36, 37], and surface plasmon resonance (SPR).

Localized surface plasmon resonance (LSPR) is a phenomenon observed when light is incident on the AgNP structure and electrons are stimulated to the induction band where they can transfer between metal boundaries and dielectric media [38]. This phenomenon occurs around the outer shell of the AgNPs because the light from the outside cannot penetrate into the material. Many pieces of research have investigated the application of nanoparticles to H_2O_2 detection [39-41] because nanoparticles have high surface-to-volume ratios resulting in a high ability to absorb light and an ability to be modified to enhance colloidal stability [42]. AgNPs are cost effective, so they are suitable for use as sensors.

This research aimed at designing a process for the green synthesis of AgNPs using the serum of SNRL after rubber coagulation with chitosan in acetic acid solution. It began with serum preparation followed by a study of the effects of process parameters on AgNP synthesis and the application of AgNPs to H_2O_2 sensing in a range of concentrations under chosen experimental conditions.

2. Materials and methods

2.1 Materials

The SNRL as a source of reducing agent was supplied by Thai Eastern Group Holding Co. Ltd. The SNRL contained 3.8 wt % DRC and 0.7 wt % ammonia. Chitosan (CS) as a rubber coagulant was purchased from the A.N. Lab Aquatic Nutrition. It possessed 98.6% degree of deacetylation (%DD) and an average molecular weight of 324,374 Da. Silver nitrate ($AgNO_3$) as a silver ion precursor, sodium hydroxide (NaOH), hydrogen peroxide (H_2O_2), and acetic acid (CH_3COOH) were supplied by Merck Ltd., Germany. Polyethylene glycol (PEG) with an average molecular weight of 6000 was supplied by Sigma-Aldrich. Phosphate buffer solution (PBS) was supplied by Amresco®.

2.2 Serum preparation and synthesis of AgNPs

Chitosan (4g) was dissolved in 400 mL of 3 vol % acetic acid solution to obtain a homogeneous CS solution at 1% w/v. The solution was then mixed with 500 mL of SNRL. After thoroughly stirring and setting aside, phase separation of rubber coagulum and the serum took place. The rubber coagulum was removed by filtering twice through a piece of filter cloth and once through a piece of nylon cloth.

The serum was diluted with distilled water in a ratio of serum volume to water volume of 1:2 before use. Two appropriate amounts of $AgNO_3$ powder were added separately to beakers of the serum and the solution mixed homogeneously until the $AgNO_3$ was completely dissolved to obtain mixtures with concentrations of silver ions of 1 mM and 3 mM. To each glass bottle, the diluted serum was added together with $AgNO_3$ solution. After that, NaOH solutions with concentrations of 0.1, 0.25, 0.5, 1.0, and 2.0 M were added separately to the mixture in each bottle and it was heated in a microwave with a power at 80 W for 15 s.

2.3 Characterization of AgNPs

The LSPR of AgNPs could be observed by UV-vis spectrophotometry (Ultrospec 2100 pro, Biochem Ltd., Cambridge, UK) in the range 360-660 nm. The AgNP colloids were then centrifuged at 13,500 rpm for 10 min to separate the particles from the liquid. They were washed with distilled water by using a vortex mixer, centrifuged again and collected and kept for examination by TEM. The analyses were performed by using a Jem-2100PLUS, JEOL instrument operated at 30 kV, 150 kV, 1.0 MV, and 1.2 MV. The images obtained by TEM were analyzed for AgNP morphology and the average size and size distributions obtained from at least 100 particles for each sample.

2.4 Detection of H_2O_2

The H_2O_2 detection experiment was conducted using diluted silver nanocolloids. The obtained AgNP colloids were separated from the serum by centrifuging at 8000 rpm for 30 min. The precipitates were removed from the supernatant and mixed with distilled water using a vortex mixer to wash the AgNPs. The washing water was finally removed from the AgNPs as a supernatant after the liquid colloids were centrifuged at 8000 rpm for 30 min. The purified AgNPs were then redispersed in distilled water at a very low concentration by ensuring that the absorbance peak was around 1.0 for the purpose of quantitative analysis. To enhance the stability of the AgNP colloids, PEG solutions were prepared at 1 and 5% w/v and used as dispersing agents when redispering the AgNPs after washing.

The H_2O_2 solutions were prepared from 30% H_2O_2 solution by dilution with PBS buffer solution (pH 7.4) to obtain concentrations in the range of 0.0625 to 0.5 mM. When applied to H_2O_2 sensing, the AgNP colloids were placed in a cuvette and mixed with H_2O_2 solution in a ratio of 4:1. The whole range of absorbance spectra was recorded from 360 to 660 nm using the UV-vis spectrophotometer at room temperature. The reaction between H_2O_2 and AgNPs was left for 10, 30 and 60 min prior to absorbance measurement.

3. Results and discussion

3.1 Characterization of AgNPs

When mixing $AgNO_3$ solution and serum together, no reaction of Ag^+ to form Ag^0 was observed, even upon heating in a microwave. The color of the solution was still clear yellow, which was the original color of the serum. It was expected that Ag^+ could form complex ions in the network of chitosan chains where the ions became embedded [43-45]. To free Ag^+ from the complex, deprotonation of chitosan using a basic solution could be an alternative.

After adding NaOH to the solution, the color of the solution changed quickly to brown, implying the emergence of AgNPs. The free Ag^+ ions now could react with sugars or other organic molecules acting as reducing agents and become seeds of the AgNPs as shown in Eq. (3.2). It should also be noted that Ag^+ could also be converted to Ag_2O precipitate in a basic solution [46], through Eqs. (3.3) and (3.4). However, only metallic nanoparticles such as AgNPs could show the effect of SPR. There is a proposed model of seed-mediated growth of nanoparticles through the formation of hydroxylated compounds [47], and these compounds could help control the size of growing nanoparticles such that it is possible that under basic conditions, after Ag^0 seeds were formed, the growth could be facilitated via the formation of AgOH before undergoing growth steps to form particles in nanoscale:

$$AgNO_3 \rightleftharpoons Ag^+ + NO_3^- \quad (1)$$

$$Ag^+ + e^- \rightleftharpoons Ag^0 \quad (2)$$

$$Ag^+ + OH^- \rightleftharpoons AgOH \quad (3)$$

$$2Ag^+(aq) + 2OH^-(aq) \rightleftharpoons Ag_2O(s) + H_2O(l) \quad (4)$$

Figure 1(a) shows the appearance of a strong and sharp LSPR band at the wavelength of maximum absorbance (λ_{max}) in the range of 403-419 nm, corresponding to the characteristic peak of AgNPs reported in the literature [48, 49]. It can be observed from Figure 1(a) that when NaOH concentration is increased from 0.1 to 1 M, the intensity of the absorbance peak increased, indicating greater numbers of particles generated and their growths controlled by hydroxylated compounds indicated by the shift of the peak (λ_{max}) to the lower wavelength. It is reported theoretically and experimentally that the size and shape of nanoparticles affect the absorbance band in LSPR; i.e., a blueshift occurs with an increase in the size of nanoparticles [50]. However, the discrepancy was seen when using 2 M NaOH solution. The λ_{max} was located at the same wavelength of 403 nm as that of 1 M NaOH sample, but the maximum intensity was lower, probably because the smaller particles may coalesce during the growth due to greater numbers of hydroxylated compounds, resulting in no contribution of smaller particles to the LSPR. This lowering of the maximum intensity at 2 M NaOH could be attributable to the precipitation of AgNP agglomerates, as the population of AgNPs was so concentrated that colloidal stability was weakened.

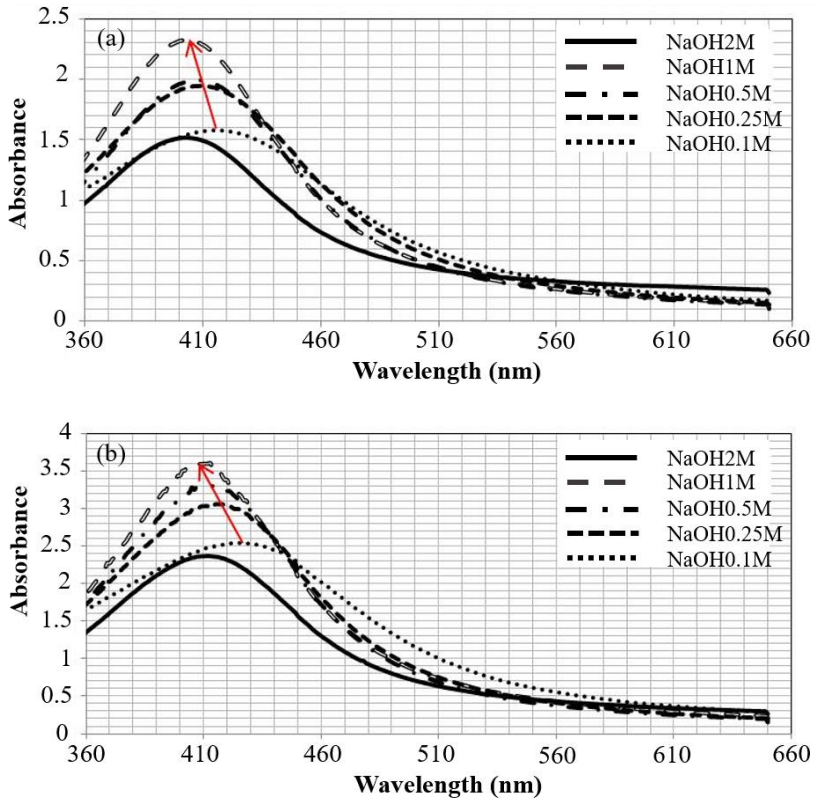

Figure 1 The effect on LSPR results of NaOH concentration varying from 0.1 to 2 M of AgNPs prepared by (a) 1 mM $AgNO_3$ solution and (b) 3 mM $AgNO_3$ solution.

According to the concept of double layer interaction, in this case negative ions of OH^- could be absorbed onto AgNPs, inducing the formation of a compact inner layer of positive ions and a diffuse outer layer of negative ions. More negative ions of OH^- could expand the overall layers, preventing the aggregation of particles. The repulsive interactions could be implied from the zeta potential of the AgNP colloids, which is reported to be more negative when the pH is adjusted to be higher in the basic range [51]. However, if the number of AgNPs is very large, while the number of OH^- ions is not enough to generate large layers around the particles, the colloidal stability could be collapsed easily if there are more chances for particles to collide with one another; this is when the density of AgNPs in the system is very high at 2 M NaOH. Besides, when comparing the absorbance spectra of stable AgNP colloids freshly synthesized and those of samples left for 1, 3, 4 and 7 days, it was found that the peak remained at the same wavelength, indicating that the average size of the AgNPs did not change over storage time, consistent with the results reported by Popaitoon and Pootrakulchote [24].

When increasing the concentration of $AgNO_3$ to 3 mM while maintaining the concentration of the serum and adjusting with NaOH at different concentrations of 0.1, 0.25, 0.5, 1, and 2 M, the LSPR results obtained are shown in Figure 1(b). The appearance of λ_{max} was observed in the range of 409-426 nm, higher than the samples prepared with 1 mM $AgNO_3$. For the same NaOH concentration, the intensity of the absorbance peak in Figure 1(b) was higher than that in Figure 1(a), indicating that higher numbers of AgNPs were produced when the concentration of Ag^+ precursor was higher. The effect of increasing NaOH discussed earlier was confirmed again in Figure 1(b).

Three samples of AgNP colloids were selected based on clear differences in λ_{max}. They were the samples prepared from 1 mM $AgNO_3$ and 1 M NaOH (denoted as 1Ag1.0Na), from 3 mM $AgNO_3$ and 1 M NaOH (denoted as 3Ag1.0Na), and from 3 mM $AgNO_3$ and 0.1 M NaOH (denoted as 3Ag0.1Na). As is evident in Figure 2, the λ_{max} values of each sample were at 405, 417 and 424 nm, respectively, implying that the average particle size of 1Ag1.0Na was smaller than that of 3Ag1.0Na, which was in turn smaller than that of 3Ag0.1Na. All AgNP samples were diluted differently to adjust their absorbance intensities to be around 1.0 in order to be used for H_2O_2 detection.

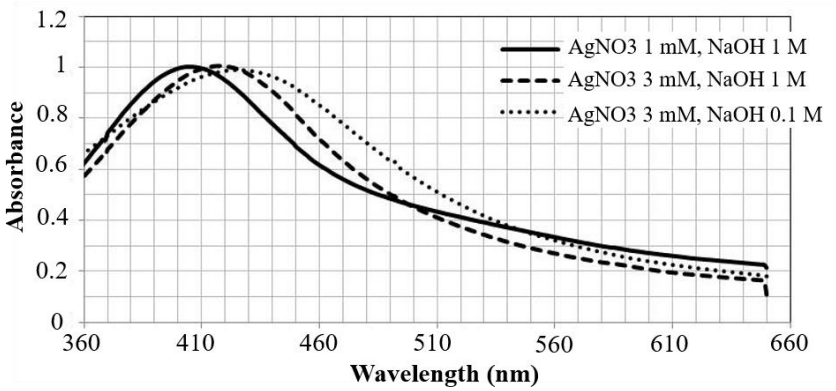

Figure 2 The LSPR results of three samples of AgNPs compared. They were all diluted to yield a maximum absorbance intensity of about 1.0.

3.2 Morphology of AgNPs

The three samples, 1Ag1.0Na, 3Ag1.0Na, and 3Ag0.1Na, were observed by TEM; the three micrographs obtained are shown in Figures 3(a), (b) and (c), respectively. The statistics were performed using at least 100 particles of each sample and the obtained average diameters were 7.942, 8.464, and 9.284 nm, respectively. Considering the size of AgNPs in the range of 6-15 nm, the percentages were 62, 98, and 99%, respectively. Both the average size and the distribution were consistent with the LSPR results. In addition, Figure 4 represents an HR-TEM image to confirm the characteristics of the Ag crystal. The *d*-spacing of the (111) plane of Ag was measured to be 0.237 nm, close to the reported standard JCPDS value of silver, which is 0.2359 nm.

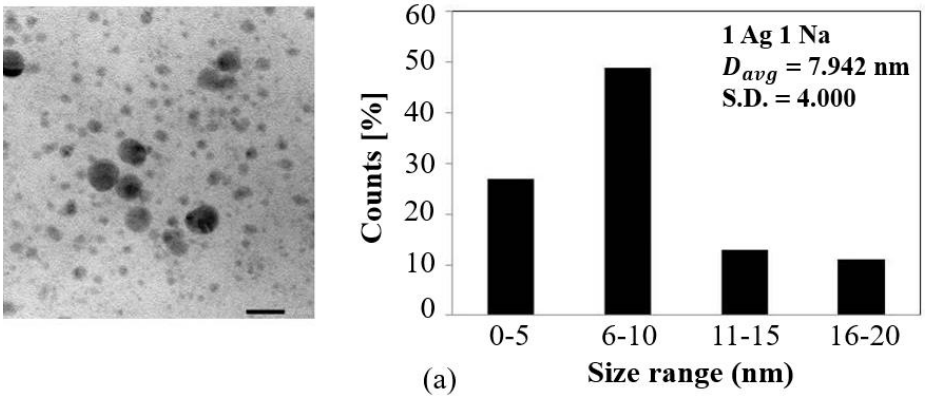

Figure 3 TEM micrographs (150K× magnification) and particle size distributions of AgNPs in the samples (a) 1Ag1.0Na (b) 3Ag1.0Na and (c) 3Ag0.1Na.

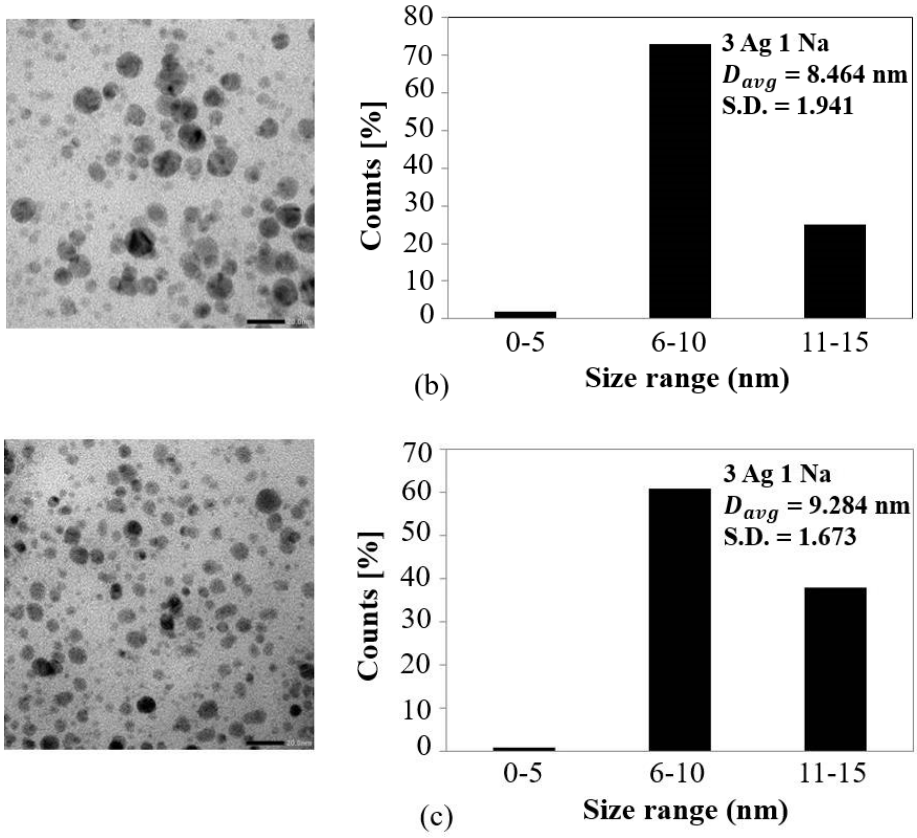

Figure 3 (continued) TEM micrographs (150K× magnification) and particle size distributions of AgNPs in the samples (a) 1Ag1.0Na (b) 3Ag1.0Na and (c) 3Ag0.1Na.

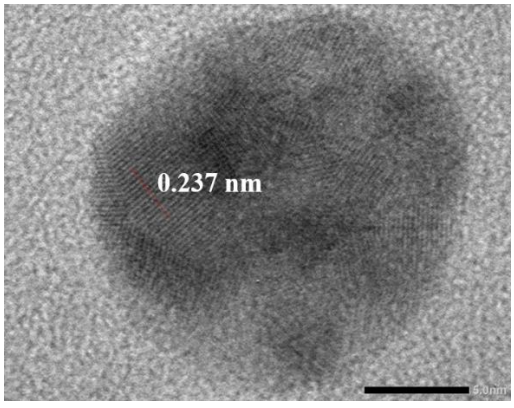

Figure 4 Micrograph (1M× magnification) from high-resolution transmission electron microscopy (HR-TEM) of 3Ag1.0 Na.

3.3 Detection of H_2O_2

Sensing H_2O_2 with AgNPs is based on the oxidation reaction between the AgNPs and H_2O_2, which is a strong oxidizing agent. Figure 5 shows the yellow color of an AgNP colloid turning lighter over time while reacting with H_2O_2 until the liquid is clear, indicating that H_2O_2 could convert Ag^0 to Ag^+ gradually over the reaction time and thereby change the LSPR results of the AgNPs.

Figure 5 The left-most bottle shows the yellow color of AgNPs before reaction. The faded samples (the other three samples) are seen after the reaction with H_2O_2 solution

As an example of LSPR changes, the results for the 3Ag0.1Na sample are displayed in Figure 6. The absorbance peak of the AgNP colloids at λ_{max} of 424 nm decreased with increasing the concentration of H_2O_2 from 0.0625 mM to 0.5 mM and shows the gradual decay of the AgNPs [39-41].

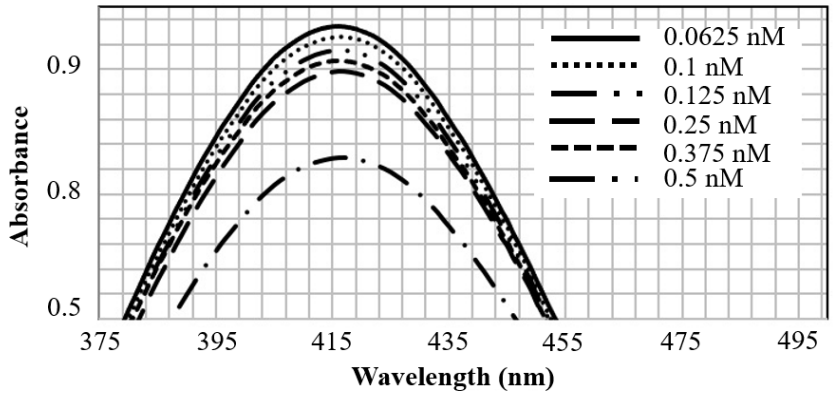

Figure 6 The LSPR results of the 3Ag0.1Na sample, showing the decreasing intensity at the peak after AgNP colloids reacted with H_2O_2 at different concentration for 30 min, indicating that they could be applied in H_2O_2 detection.

3.3.1 The effect of reaction time

To apply the decay of absorbance peak as a function of H_2O_2 concentration to H_2O_2 detection, the reaction time has to be chosen, and the stability of the AgNP colloids has to be investigated. Initially, the results at different reaction times were evaluated using the 3Ag0.1Na sample with no stabilizing agent.

Figures 7(a), (b), and (c) show the plot of maximum absorbance intensity versus H_2O_2 concentration at different reaction times of 10, 30 and 60 min, respectively. Some studies have reported the linear relation between maximum absorbance intensity and H_2O_2 concentration [40, 42], which is possible when the concentration range is narrow, whereas some have reported the linear relation between the former and the logarithmic function of the latter [39, 41], which is more appropriate when the concentration range is wide. For this study, both types of plot were constructed, and it was found that values of correlation coefficient, R^2, of both were comparable. The linear plot was then adopted here to represent our data and is used throughout this study.

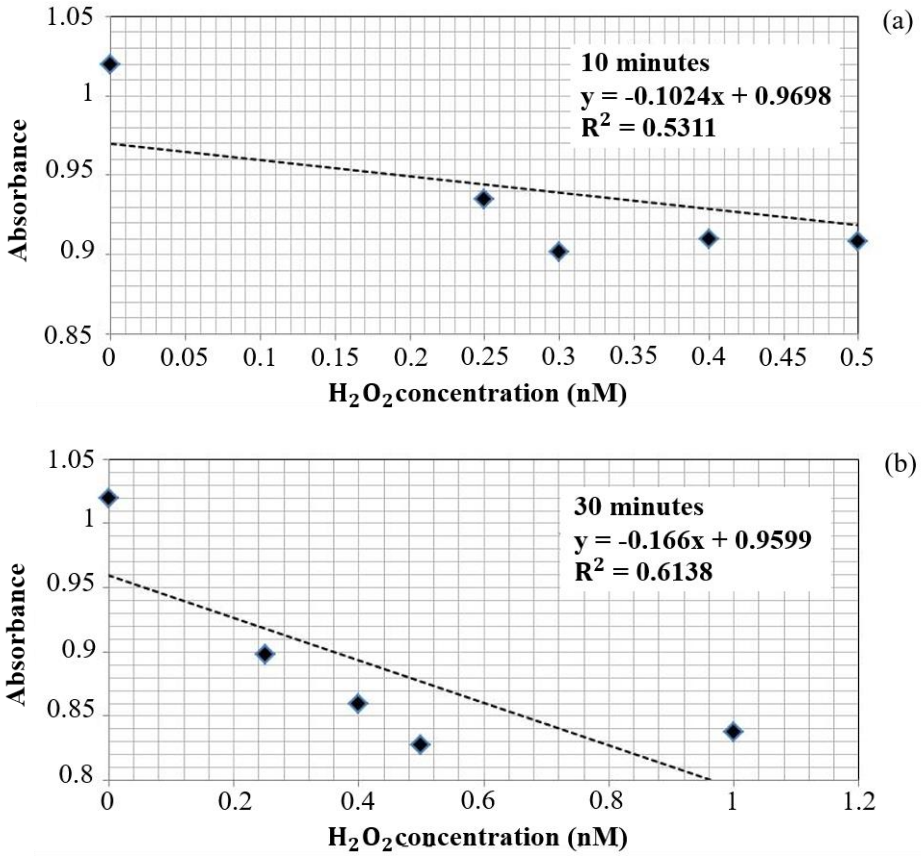

Figure 7 The maximum absorbance changes for AgNPs reacting with H_2O_2 at different concentrations and for different reaction time of (a) 10 min, (b) 30 min and (c) 60 min.

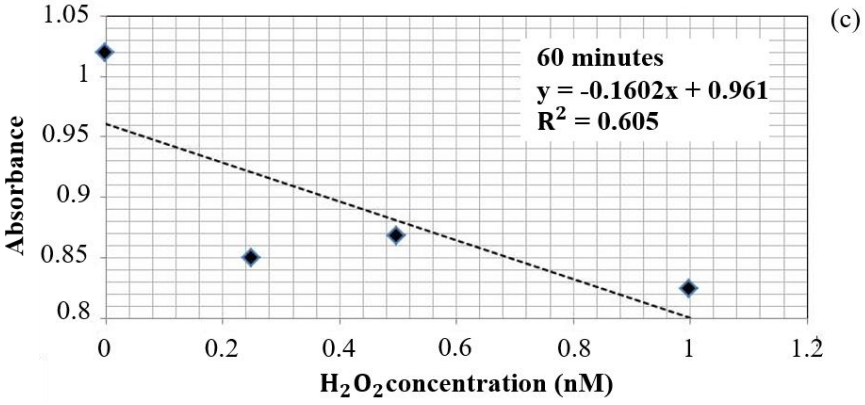

Figure 7 (continued) The maximum absorbance changes for AgNPs reacting with H_2O_2 at different concentrations and for different reaction time of (a) 10 min, (b) 30 min and (c) 60 min.

All plots gave low values of R^2, indicating that the stability of AgNP colloids alone were so low for this application that the aid of a stabilizing agent was needed. The decrease in AgNP stability was due to the dilution of the obtained AgNP colloid with PBS to yield an LSPR peak absorbance of around 1.0. The concentration of hydroxide ions that help stabilize the colloids was also decreased. However, all plots still gave a useful result regarding the reaction time. Considering the slopes of the linear fittings, which were -0.1024, -0.166 and -0.1602 for 10, 30 and 60 min, respectively, it could be stated that the sensitivity of AgNPs when applied at 30 min was significantly better than at 10 min and not much different at 60 min. Based on this experiment, the reaction of 30 min was chosen for subsequent experiments.

3.3.2 The effect of the stabilizing agent

The stabilizing agent chosen in this study was polyethylene glycol (PEG6000), since it is water-soluble, nontoxic and could act as a surfactant. Usually, the enhancement of colloidal stability by increasing repulsions between colloidal particles could be accomplished by either electrostatic or steric effects, of which the latter is the case for PEG. PEG chains could adsorb onto AgNP surfaces causing steric repulsions and preventing aggregations of very fine nanoparticles so that the AgNP could distribute uniformly in colloids. Since sensing is based on the heterogeneous reaction of H_2O_2 molecules with silver atoms on the AgNP surfaces, the reaction could proceed effectively when the particles are distributed uniformly.

The appropriate amount of PEG to use was tested by using concentrations of PEG of 1 and 5% wt/v. The PEG solution was used first to dilute the AgNP colloids. The 3Ag0.1Na sample was used to react with H_2O_2 at various concentrations from 0.0625 mM to 0.5 mM. The results are shown in Figures 8(a), (b) and (c) for no PEG, 1% wt/v PEG and 5% wt/v PEG, respectively. The value of R^2 increased from 0.3745 to 0.9573 and to 0.9906 when increasing the concentration of PEG from 0 to 1 and to 5% wt/v respectively, indicating that PEG could stabilize AgNPs more effectively up to 5% wt/v.

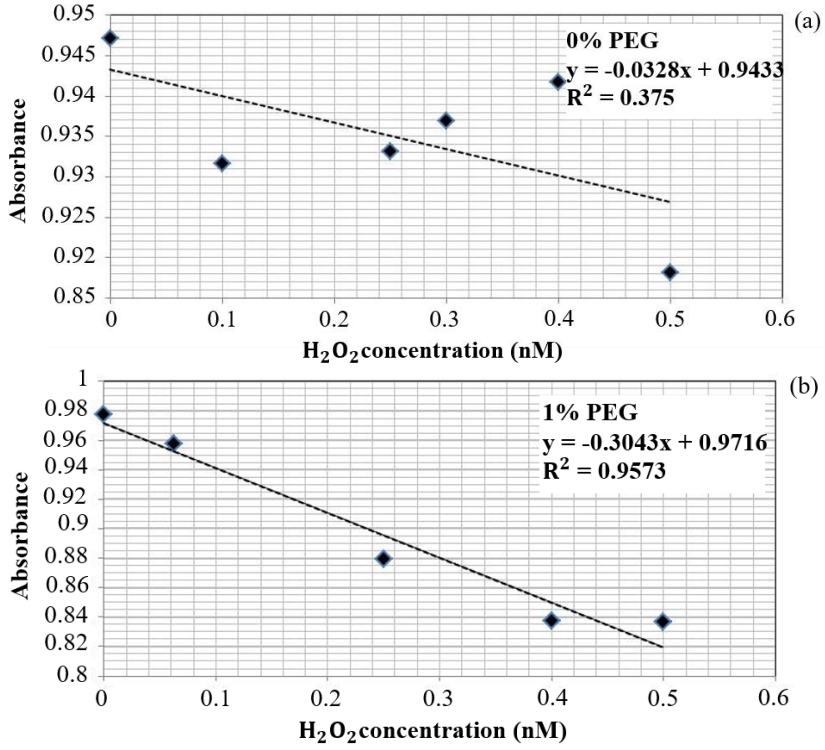

Figure 8 The effect of PEG at different concentrations: (a) 0% wt/v PEG, (b) 1% wt/v PEG and (c) 5% wt/v PEG, to stabilize the 3Ag1.0Na sample.

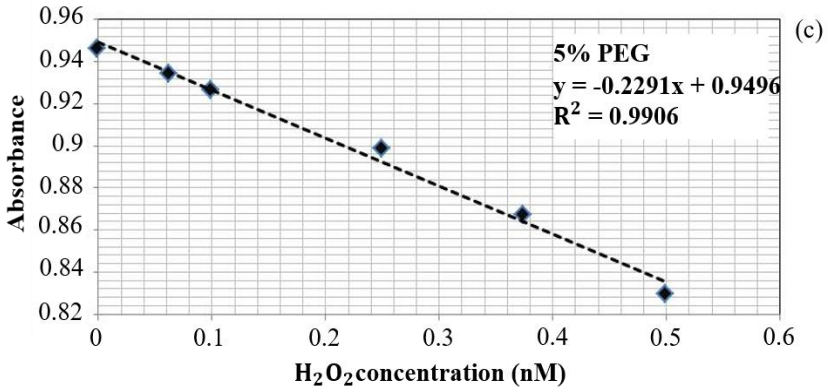

Figure 8 (continued) The effect of PEG at different concentrations: (a) 0% wt/v PEG, (b) 1% wt/v PEG and (c) 5% wt/v PEG, to stabilize the 3Ag1.0Na sample.

3.3.3 The effect of AgNP characteristics

The final experiment involved three different samples of AgNPs, as discussed earlier in Section 3.1. All samples were diluted with 5% wt/v PEG and reacted with H_2O_2 at various concentrations from 0.0625 mM to 0.5 mM. The three colloids were 1Ag1.0Na, 3Ag1.0Na and 3Ag0.1Na, which corresponded to values of λ_{max} of 405, 417, and 424 nm, respectively. After reaction for 30 min, the results were obtained and plotted as shown in Figures 9(a), (b) and 8(c) for the samples 1Ag1.0Na, 3Ag0.1Na and 3Ag1.0Na, respectively.

The linear response to H_2O_2 of all AgNP colloidal samples is clearly observed with values of R^2 of 0.9721, 0.9906, and 0.7216 and slopes of 0.2029, 0.2291 and 0.0776, respectively. As expected, the different sizes of the nanoparticles affected their ability to measure H_2O_2 concentration. Considering both R^2 and slope, it seemed that the sample 3Ag1.0Na was the sensor with the best consistency in linear response in this fixed range of H_2O_2 concentration and the best sensitivity to differentiate samples of concentrations in a narrow range. This best performance might be attributable to the fact that the sizes of the particles were not too great and the improvement in stability was effective. It was quite apparent that the sample with the largest particles, 3Ag0.1Na, was the least sensitive. The sample of smallest size, 1Ag1.0Na, was expected to be the best but turned out to be the second-best, implying that 5% wt/v PEG might be specific for 3Ag1.0Na, but not for 1Ag1.0Na. The percentage of PEG might need to be fine-tuned for the finer particles.

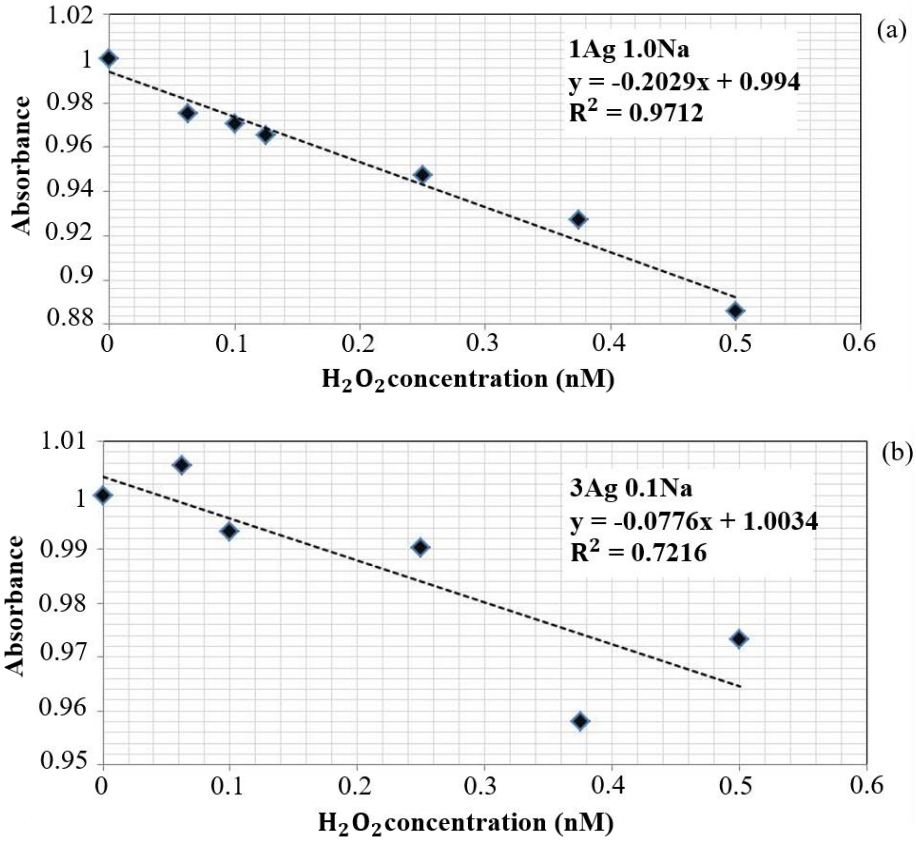

Figure 9 The linear responses of different AgNP samples: (a) 1Ag1.0Na and (b) 3Ag0.1Na used for detection of H_2O_2 at 30 min.

4. Conclusions

The synthesis of AgNPs using serum from SNRL obtained by coagulation with chitosan and acetic acid was successfully carried out. For all experimental conditions, the size of the obtained AgNPs was <19 nm, with a mean average size of <10 nm. The decrease in AgNP size depends on a decrease in AgNO3 concentration and an increase in NaOH concentration. The synthesized AgNPs were later applied for H_2O_2 detection. The experimental results indicated that not only the size of the AgNPs but also their stability played important roles in chemical sensing. PEG at 5% wt/v was necessary to stabilize the AgNP colloids before use. The AgNPs of small sizes yielded high sensitivity provided that the colloidal stability was adequate. However, the AgNPs obtained could be applied in a wide range of applications that should be investigated in the future. This research showed the potential use of SNRL as a sustainable source of reducing agents for metallic nanoparticle production.

5. Acknowledgments

Financial support with the contract number 005/2563 from the Faculty of Engineering, Thammasat University for the fiscal year 2020 is gratefully acknowledged.

6. References

[1] Gopinath K, Kumaraguru S, Bhakyaraj K, Mohan S, Venkatesh KS, Esakkirajan M, et al. Green synthesis of silver, gold and silver/gold bimetallic nanoparticles using the Gloriosa superba leaf extract and their antibacterial and antibiofilm activities. Microb Pathog. 2016;101:1-11.
[2] Lomeli-Marroquin D, Cruz DM, Nieto-Arguello A, Crua AV, Chen J, Torres-Castro A, et al. Starch-mediated synthesis of mono- and bimetallic silver/gold nanoparticles as antimicrobial and anticancer agents. Int J Nanomed. 2019;14:2171-90.
[3] Ravichandran V, Vasanthi S, Shalini S, Shah SA, Tripathy M, Paliwal N. Green synthesis, characterization, antibacterial, antioxidant and photocatalytic activity of Parkia sp eciosa leaves extract mediated silver nanoparticles. Results Phys. 2019;15:102565.
[4] Parial D, Patra HK, Roychoudhury P, Dasgupta AK, Pal R. Gold nanorod production by cyanobacteria-a green chemistry approach. J App. Phycol. 2012;24:55-60.
[5] Katas H, Lim CS, Azlan AY, Buang F, Busra MF. Antibacterial activity of biosynthesized gold nanoparticles using biomolecules from Lignosus rhinocerotis and chitosan. Saudi Pharm J. 2019;27:283-92.
[6] Thangamani N, Bhuvaneshwari N. Green synthesis of gold nanoparticles using Simarouba glauca leaf extract and their biological activity of micro-organism. Chem Phys Lett. 2019;732:136587.
[7] Ullah N, Odda AH, Li D, Wang Q, Wei Q. One-pot green synthesis of gold nanoparticles and its supportive role in surface activation of non-woven fibers as heterogeneous catalyst. Colloids Surf A. 2019;571:101-9.
[8] Pandian CJ, Palanivel R, Dhananasekaran S. Green synthesis of nickel nanoparticles using Ocimum sanctum and their application in dye and pollutant adsorption. Chin J Chem Eng. 2015;23:1307-15.
[9] Pandian CJ, Palanivel R, Balasundaram U. Green synthesized nickel nanoparticles for targeted detection and killing of S. typhimurium J Photochem Photobiol B. 2017;174:58-69.
[10] Liaskovska M, Tatarchuk T, Bououdina M, Mironyuk I. Green synthesis of magnetic spinel nanoparticles. In: Fesenko O, Yatsenko L, editors. Proceedings of the 6th International Conference Nanotechnology and Nanomaterials (NANO2018); 2018 Aug 27-30; Kyiv, Ukraine. Berlin: Springer; 2019. p. 389-98.
[11] Bibi I, Nazar N, Ata S, Sultan M, Ali A, Abbas A, et al. Green synthesis of iron oxide nanoparticles using pomegranate seeds extract and photocatalytic activity evaluation for the degradation of textile dye. J Mater Res Tech. 2019;8:6115-24.
[12] Mohammadlou M, Maghsoudi H, Jafarizadeh-Malmiri HJ. A review on green silver nanoparticles based on plants: synthesis, potential applications and eco-friendly approach. Int Food Res J. 2016;23:446-63.
[13] Vasileva P, Donkova B, Karadjova I, Dushkin C. Synthesis of starch-stabilized silver nanoparticles and their application as a surface plasmon resonance-based sensor of hydrogen peroxide. Colloids Surf A. 2011;382:203-10.
[14] Halkai KR, Mudda JA, Shivanna V, Rathod V, Halkai R. Biosynthesised silver nanoparticles from fungi as antimicrobial agents for endo-perio lesions-A review. Annu Res Rev Biol. 2016;10:1-7.
[15] Lee SH, Jun BH. Silver nanoparticles: synthesis and application for nanomedicine. Int J Mol Sci. 2019;20:865-88.
[16] Garibo D, Borbon-Nunez HA, de Leon JN, Mendoza EG, Estrada I, Toledano-Magana Y, et al. Green synthesis of silver nanoparticles using Lysiloma acapulcensis exhibit high-antimicrobial activity. Sci Rep. 2020;10:12805.
[17] Jebril S, Jenana RK, Dridi C. Green synthesis of silver nanoparticles using Melia azedarach leaf extract and their antifungal activities: In vitro and in vivo. Mater Chem Phys. 2020;248:122898.
[18] Alkhalaf MI, Hussein RH, Hamza A. Green synthesis of silver nanoparticles by Nigella sativa extract alleviates diabetic neuropathy through anti-inflammatory and antioxidant effects. Saudi J Biol Sci. 2020;27:2410-9.
[19] Saleh GM, Najim SS. Antibacterial activity of silver nanoparticles synthesized from plant latex. Iraqi J Sci. 2020;61:1579-88.
[20] Perrella FW, Gaspari AA. Natural rubber latex protein reduction with an emphasis on enzyme treatment. Meth. 2002;27:77-86.
[21] Eng AH, Ong EL. Hevea natural rubber. In: Bhowmick AK, Stephens HL, editors. Handbook of elastomers. Plastics engineering series. New York: CRC Press; 2000. p. 29-59.
[22] Suwatthanarak T, Than-ardna B, Danwanichakul D, Danwanichakul P. Synthesis of silver nanoparticles in skim natural rubber latex at room temperature. Mater Lett. 2016;168:31-5.
[23] Danwanichakul P, Suwatthanarak T, Suwanvisith C, Danwanichakul D. The role of ammonia in synthesis of silver nanoparticles in skim natural rubber latex. J Nanosci. 2016;2016:7258313.
[24] Popaitoon N, Pootrakulchote N. Synthesis of silver nanoparticles in skim natural rubber for dye-sensitized solar cell. Journal of King Mongkut's University of Technology North Bangkok. 2018;28(1):183-90.
[25] Moonprasith N, Loykulnant S, Kongkaew C. Use of hydroxypropylmethylcellulose as thermo-responsive flocculant in skim natural rubber latex. Adv Mater Res. 2008;55:913-6.
[26] Pongsanon P, Danwanichakul P. The synthesis of gold nanoparticles by using skim natural rubber latex and the recycling of remaining reactants. Thai Sci Tech J. 2020;28:596-606.

[27] Vo KD, Guillon E, Dupont L, Kowandy C, Coqueret X. Influence of Au (III) interactions with chitosan on gold nanoparticle formation. J Phys Chem C. 2014;118:4465-74.
[28] Danwanichakul P, Werathirachot R, Kongkaew C, Loykulnant S. Coagulation of skim natural rubber latex using chitosan or polyacrylamide as an alternative to sulfuric acid. Eur J Sci Res. 2011;62:537-47.
[29] Sanchez J, Myers TN. Peroxides and peroxide compounds, organic peroxides. Kirk-Othmer Encyclopedia of Chemical Technology. USA: Wiley; 2000.
[30] Beltran FJ, Encinar J, Gonzalez JF. Industrial wastewater advanced oxidation Part 2. Ozone combined with hydrogen peroxide or UV radiation. Water Res. 1997;31:2415-28.
[31] Badmus MA, Audu TO, Anyata BU. Removal of heavy metal from industrial wastewater using hydrogen peroxide. Afr J Bio tech. 2007;6:238-42.
[32] Teong SP, Li X, Zhang Y. Hydrogen peroxide as an oxidant in biomass-to-chemical processes of industrial interest. Green Chem. 2019;21:5753-80.
[33] Zhang Q, Fu S, Li H, Liu Y. A novel method for the determination of hydrogen peroxide in bleaching effluents by spectroscopy. BioResources. 2013;8:3699-705.
[34] Guo JZ, Cui H, Zhou W, Wang W. Ag nanoparticle-catalyzed chemiluminescent reaction between luminol and hydrogen peroxide. J Photochem Photobiol A. 2008;19:89-96.
[35] Han JH, Jang J, Kim BK, Choi HN, Lee WY. Detection of hydrogen peroxide with luminol electrogenerated chemiluminescence at mesoporous platinum electrode in neutral aqueous solution. J Electroanal Chem. 2011;660:101-7.
[36] Chen W, Cai S, Ren QQ, Wen W, Zhao YD. Recent advances in electrochemical sensing for hydrogen peroxide: a review. Analyst. 2012;137:49-58.
[37] Chen S, Yuan R, Chai Y, Hu F. Electrochemical sensing of hydrogen peroxide using metal nanoparticles: a review. Microchim Acta 2013;180:15-32.
[38] Cobley CM, Skrabalak SE, Campbell DJ, Xia Y. Shape-controlled synthesis of silver nanoparticles for plasmonic and sensing applications. Plasmonics. 2009;4:171-9.
[39] Zhang L, Li L. Colorimetric detection of hydrogen peroxide using silver nanoparticles with three different morphologies. Anal Meth. 2016;8:6691-5.
[40] Nguyen ND, Van Nguyen T, Chu AD, Tran HV, Tran LT, Huynh CD. A label-free colorimetric sensor based on silver nanoparticles directed to hydrogen peroxide and glucose. Arabian J Chem. 2018;11:1134-43.
[41] Teodoro KB, Migliorini FL, Christinelli WA, Correa DS. Detection of hydrogen peroxide (H_2O_2) using a colorimetric sensor based on cellulose nanowhiskers and silver nanoparticles. Carbohydr Polym. 2019;212:235-41.
[42] Vasileva P, Donkova B, Karadjova I, Dushkin C. Synthesis of starch-stabilized silver nanoparticles and their application as a surface plasmon resonance-based sensor of hydrogen peroxide. Colloids Surf A. 2011;382:203-10.
[43] Bozanic DK, Trandafilovic LV, Luyt AS, Djokovic V. 'Green'synthesis and optical properties of silver-chitosan complexes and nanocomposites. React Funct Polym. 2010;70:869-73.
[44] Venkatesham M, Ayodhya D, Madhusudhan A, Babu NV, Veerabhadram G. A novel green one-step synthesis of silver nanoparticles using chitosan: catalytic activity and antimicrobial studies. Appl Nanoscience. 2014;4:113-9.
[45] Wongpreecha J, Polpanich D, Suteewong T, Kaewsaneha C, Tangboriboonrat P. One-pot, large-scale green synthesis of silver nanoparticles-chitosan with enhanced antibacterial activity and low cytotoxicity. Carbohydr Polym. 2018;199:641-8.
[46] Manyuan N, Kempet S. Coating of gold nanoparticles synthesized from spent coffee ground extract and their colloidal stability [undergraduate thesis]. Pathumtani: Thammasat University; 2019.
[47] Agunloye, Panariello, Gavriilidis, Mazzei. A model for the formation of gold nanoparticles in the citrate synthesis method. Chem Eng Sci. 2018;191:318-31.
[48] Kamat PV, Flumiani M, Hartland GV. Picosecond dynamics of silver nanoclusters. Photoejection of electrons and fragmentation. J Phys Chem B. 1998;102:3123-8.
[49] Mulfinger L, Solomon SD, Bahadory M, Jeyarajasingam AV, Rutkowsky SA, Boritz C. Synthesis and study of silver nanoparticles. J Chem Educ. 2007;84:322-5.
[50] Cao J, Sun T, Grattan KT. Gold nanorod-based localized surface plasmon resonance biosensors: a review. Sens Actuators B. 2014;195:332-51.
[51] He W, Zhou YT, Wamer WG, Boudreau MD, Yin JJ. Mechanisms of the pH dependent generation of hydroxyl radicals and oxygen induced by Ag nanoparticles. Biomaterials. 2012;33:7547-55.